

An Experimental Method to Estimate the Growth-rate of a Leaf using Image Processing and solving an Inverse-Growth-Problem

Geetanjali Chakravorty, Ramnath Babu T J, Sunkara Preethi, Utpal Nath,
G.K. Ananthasuresh
Indian Institute of Science, Bangalore, India

Abstract

Plant leaves provide a convenient model system to study growth in living organisms and to investigate controlled growth for achieving a design objective. In this work, we describe geometric and kinematic aspects of estimating the growth-rate in a leaf. We use an image-processing technique in conjunction with time-lapse imaging of a spotted leaf and solving an inverse problem in growth. Geometry and kinematics are inherent in this problem.

We describe a leaf-growth experimental setup in which the leaves under consideration are first marked with dots and the evolution of their form is tracked by photographing the leaves. We then subject these images to image-processing operations namely image-perspective alignment followed by suitable scaling. The locations of markers in these images are then extracted with an accuracy of 100 microns, from which the intermediate growth-displacements are computed. These displacements are specified as input to the inverse problem, wherein the nodal coordinates of the initial and grown configurations are specified and the growth-rate required to effect the growth is estimated. The results of the experiments run in-house and the key insights are presented.

Keywords: Inverse problem, growth, image processing

1 Introduction

In mechanics, the inverse growth problem entails the determination of the growth-rate in a growing body, which when induced in a growing body, will make it grow to attain a desired final form [1]. This is illustrated with an example in Fig. (1). We are given the initial configuration Ω_i and the target displacements, specified throughout

Geetanjali Chakravorty

Department of Mechanical Engineering, IISc Bangalore, E-mail:geeta@mecheng.iisc.ernet.in

Ramnath Babu T J

Department of Mechanical Engineering, IISc Bangalore, E-mail:ramnath@mecheng.iisc.ernet.in

Sunkara Preethi

Department of Molecular and Cell Biology, IISc Bangalore, E-mail:preethi@mcbl.iisc.ernet.in

Utpal Nath

Department of Molecular and Cell Biology, IISc Bangalore, E-mail:utpal@mcbl.iisc.ernet.in

G.K. Ananthasuresh

Department of Mechanical Engineering, IISc Bangalore, E-mail:suresh@mecheng.iisc.ernet.in

the domain or at particular nodes inside the domain, which capture the desired final form Ω_f . Using the inverse problem, we wish to estimate the growth-rate, which when induced in body Ω_i , will make it grow into Ω_f . Perspective transformation and kinematics of motion and elastic deformation are important components of this problem.

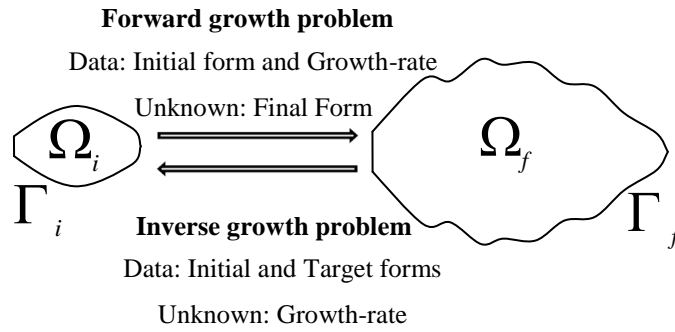


Figure 1: Illustration of the inverse problem in growth. The initial (ungrown) the final (grown) configurations are represented by Ω_i and Ω_f respectively.

The aforementioned inverse problem is studied in the context of a growing leaves, since leaves are laminar which allows us to model them as 2D structures. In this work, we present a method to estimate the growth-rate of a growing leaf using an experimental technique in conjunction with a numerical technique.

The measurement of leaf growth is based on the analysis that leaf surface is growing linearly. Temporal resolution of leaf can be done by continuous measurement of length. This was used to analyze the monocot leaf growth [2]. One more method by capturing sequences of growing leaf images analyses motion as well as growth-rate [3]. In the ‘diel leaf growth of soybean’ paper [4], artificial beads were attached to the leaf margin. In this, leaf expansion calculation is based on the increase in area of the polygon defined by the centers of mass of the beads that are attached to the leaf margin.

Apart from single leaf growth-rate measurement, there are methods which provide information about alignment as well tracking of multiple leaves [5]. Leaf alignment is the procedure which provides the information about the leaf structure by aligning all leaf images with a leaf landmark [6]. Leaf tracking provides the tracking or location information of leaves with respect to time [7].

Calculation for leaf growth-rate can be done using image processing [8]. In this method, all the leaf images are first aligned [9]. After that, leaf spots are tracked across all images. For both these methods perspective transformation plays a major role.

In this work, we present an experimental setup which in conjunction with the inverse growth problem, allows us to estimate the growth-rate in a leaf. In the following section, we describe the experimental setup.

2 Experimental Setup

The leaf-spotting experiment involves marking and tracking a grid of dots (hereafter referred to as spots) as the leaves grow. This was done on the leaves of a tobacco variant (*Nicotiana benthamiana*), which were grown in a controlled environment. Tobacco was chosen since their leaves mature fast and grow to a large size. The setup shown in Fig. (2). It consists of two fixed vertical guides supported on a base, with one horizontal guide, which can be positioned at a desired height from the base. A digital camera (Olympus SP-590UZ, CLA-11 lens) is mounted on a three degree-of-freedom (dof) XYZ positioner, which in turn can slide along the horizontal guide. This setup enables one to fix the camera in a desired orientation to capture the images of a plant which is under consideration. The image-capture experiment was performed on normal leaves that were flat. This allowed us to use a single camera to capture and record the growing 2D leaf lamina.

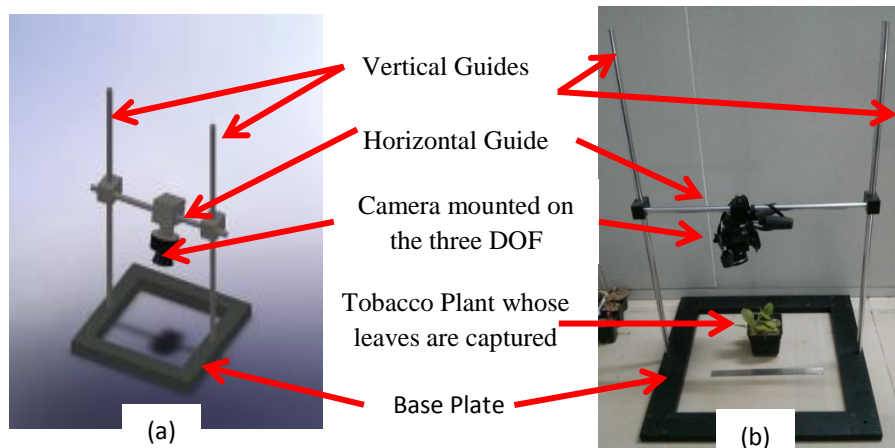


Figure 2: (a) The solid model of the device used to capture images. (b) The device with the camera mounted, oriented to face the plant that is being imaged.

A few flat leaves were identified and spotted. The upper half of the leaf was marked with a rectangular array of dots as shown in Fig. (3a). A rectangular grid was chosen since it would allow us to construct a finite element mesh, once the points are extracted. On the other half of the leaf, a rectangular label (colored paper) of known dimensions was stuck as shown in Fig. (3b). This label is used as the reference for aligning and scaling the images, as its dimensions are known and it does not expand as the leaf grows.

Snapshots of the leaves were taken every day, from six weeks from sowing, which ensured that the leaf lamina was large enough to accommodate about 100 spots (in the case presented here, we had 114 spots). The imaging was done for a period of three weeks until the leaves remained flat. These images were then processed as explained in the next section.

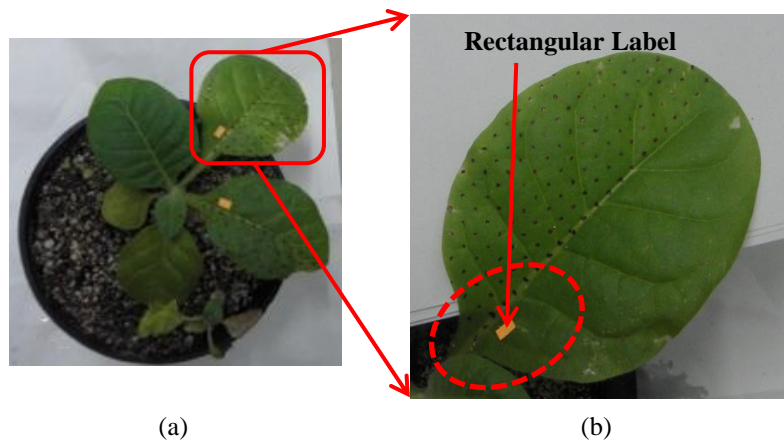


Figure 3: (a) A plant that was spotted for this experiment; and (b) zoomed-in view of a leaf showing the markers on one half of the leaf and a rectangular label that was stuck on other half which was used to align the image.

3 Image Processing

The images captured manually, need to be aligned and scaled so that the displacements of the spots can be extracted by comparing successive snapshots of the growing leaf. To achieve this, as noted earlier, we stuck rectangular markers of known dimensions ($5\text{mm} \times 3\text{mm}$ in this experiment) on the young leaf (Fig. (3a)). The various steps involved, are shown in the flowchart in Fig. (4). In this section, we describe image processing steps namely image alignment and extraction of spots.

3.1 Image alignment

Since we know that the label is rectangular and does not expand along with the leaf, the images are aligned using a suitable perspective transformation. To do this, the four corners of the rectangle viz., L_1 , L_2 , L_3 and L_4 (indicated with hollow (red) circles in Fig (5)) were manually specified for each image. The new centres of the transformed image were then computed using the following formulae:

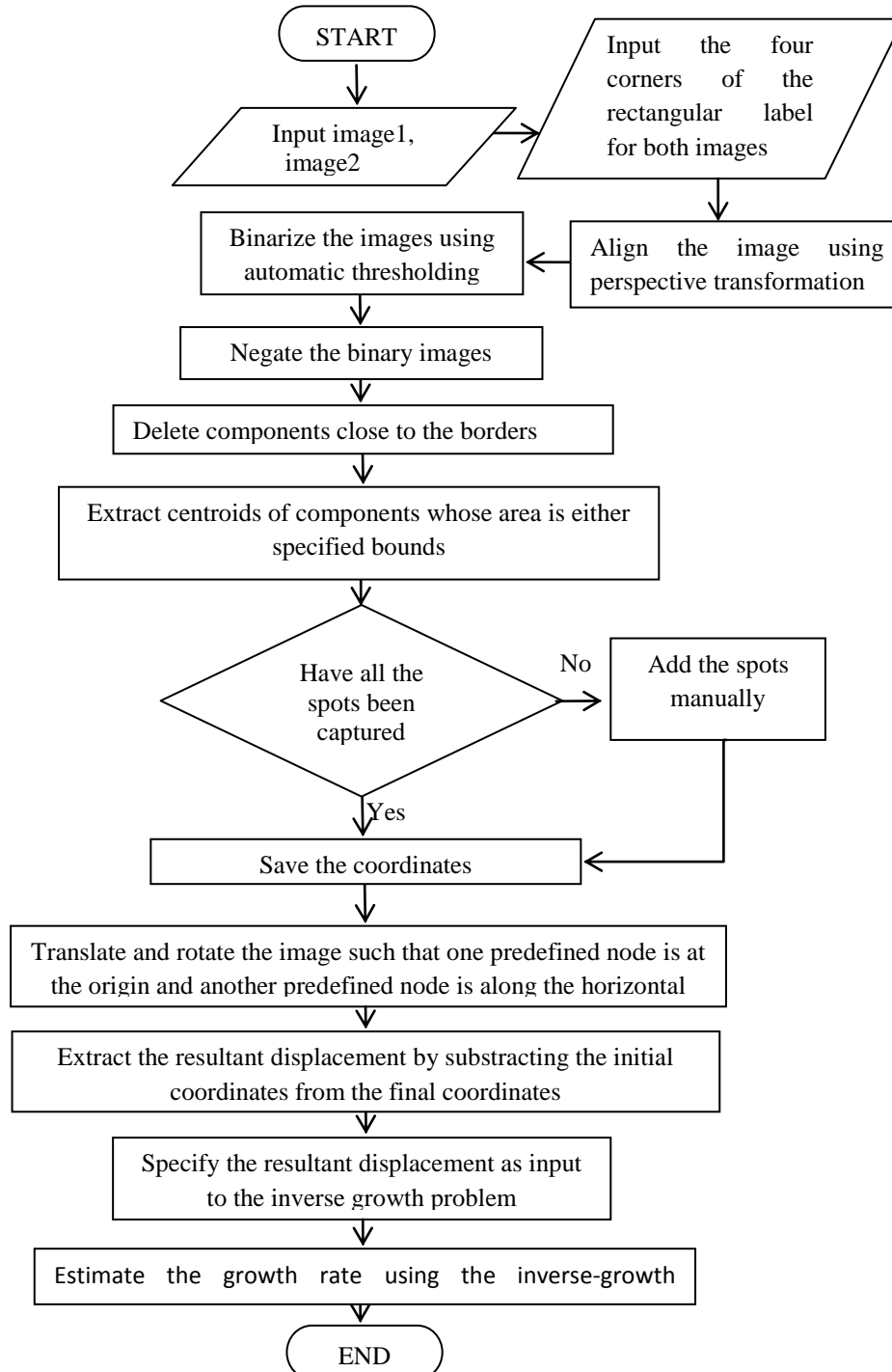


Figure 4: Flowchart of the process to estimate the growth-rate in a leaf, starting from input of images, through various steps in image-processing, followed by the inverse-growth problem

$$\begin{aligned}
C_{1x} &= (L_{1x} + L_{4x}) / 2 \\
C_{3x} &= (L_{2x} + L_{3x}) / 2 \\
C_{2y} &= (L_{1y} + L_{2y}) / 2 \\
C_{4y} &= (L_{3y} + L_{4y}) / 2
\end{aligned} \tag{1}$$

where the subscripts x and y indicate the abscissa and ordinates respectively.

Using these centres, the new corners of the aligned (corrected) rectangle A_i were obtained using the following formulae:

$$\begin{aligned}
A_1 &= (C_{1x}, C_{2y}) \\
A_2 &= (C_{3x}, C_{2y}) \\
A_3 &= (C_{3x}, C_{4y}) \\
A_4 &= (C_{1x}, C_{4y})
\end{aligned} \tag{2}$$

where the subscripts x and y indicate the abscissa and ordinates respectively and the subscript i runs from 1 to 4.

For aligning the images, we constructed a projective transformation T , that maps the initial coordinates L_i to the aligned coordinates A_i as follows:

$$\begin{bmatrix} A_{ix} \\ A_{iy} \\ 1 \end{bmatrix} = T * \begin{bmatrix} L_{ix} \\ L_{iy} \\ 1 \end{bmatrix} \quad L_i, \text{ where } 1 \leq i \leq 4 \tag{3}$$

This transformation T is a matrix of the following type:

$$T = \begin{bmatrix} A & D & G \\ B & E & H \\ C & F & I \end{bmatrix}$$

$$\begin{aligned}
A_x &= (AL_{ix} + BL_{ix} + C) / (GL_{ix} + HL_{ix} + I) \quad L_i, \text{ where } 1 \leq i \leq 4 \\
A_y &= (DL_{iy} + EL_{iy} + C) / (GL_{ix} + HL_{ix} + I)
\end{aligned} \tag{4}$$

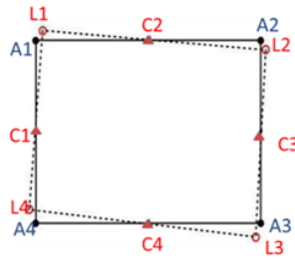


Figure 5: Picture describing how the perspective alignment of the image is done. The dotted rectangle indicates the skewed rectangle and the solid is the corresponding aligned rectangle. The (red) hollow circles L_1 , L_2 , L_3 and L_4 , represent the corners of the skewed rectangle that is obtained from the corners of the label in the image. The (blue) triangles C_1 , C_2 , C_3 and C_4 are the intermediate points which are used to then compute the new corners of the aligned rectangle A_1 , A_2 , A_3 and A_4 using the Eq. (2)

which can be computed using the Matlab function *maketform*.

Following the perspective correction of the images, each image was scaled and translated so that the labels are of the same dimensions and occupy the same position in each image. Then the difference in positions of the spots, across successive images was computed, which was specified as input in the inverse-growth problem.

4 Estimation of growth-rate

The growth-rate within the domain was estimated using the inverse growth problem. For this, we used the discretized framework for growth presented in [1], [10] and the corresponding inverse-growth problem. We pose the growth-rate estimation as a constrained minimization problem, whose formulation is presented in this section.

4.1 Formulation of the inverse growth problem in a discretized setting

The initial shape of the leaf lamina is captured using a finite element mesh, with the spots (dots) as nodes. By comparing the location of the dots between two aligned images, we obtain the displacements undergone by the dots (or the nodes). These nodal displacements are specified as target displacements in the inverse problem. The problem of estimating the growth-rate is posed as follows.

$$\begin{aligned}
 & \text{Minimize } \mathbb{E} = \frac{(\Delta \mathbf{u})^T (\Delta \mathbf{u})}{2} \\
 & \text{subject to} \\
 & \boldsymbol{\mu}: \quad \mathbf{K} \mathbf{u}_c - \mathbf{f} + \mathbf{R}^T \boldsymbol{\lambda} = \mathbf{0} \\
 & \boldsymbol{\alpha}: \quad \mathbf{R} \mathbf{u}_c - \mathbf{d} = \mathbf{0} \\
 & \boldsymbol{\gamma}: \quad 1 - \mathbf{g} \leq \mathbf{0} \\
 & \text{where } \Delta \mathbf{u} = \mathbf{u} - \mathbf{u}^* = \mathbf{u}_c + \mathbf{u}_g - \mathbf{u}^* \\
 & \text{Data: } \mathbf{u}^*, (\mathbf{u}_c)_F, (\mathbf{u}_g)_F, \mathbf{K}, \mathbf{f}_X, \mathbf{R}, \mathbf{d} \\
 & \text{Unknowns: } \mathbf{g}, (\mathbf{u}_c)_X, (\mathbf{u}_g)_X, \mathbf{f}_F, \boldsymbol{\lambda}, \boldsymbol{\mu}, \boldsymbol{\alpha}, \boldsymbol{\gamma}
 \end{aligned} \tag{5}$$

where \mathbb{E} is the objective function (the error) that is being minimized; $\Delta \mathbf{u}$ is the difference between the observed target displacement \mathbf{u}^* and the numerically computed displacement \mathbf{u} , the quantity whose square-norm is minimized using \mathbb{E} ; the numerically computed displacement \mathbf{u} is the sum of the displacement associated with the free-growth \mathbf{u}_g and the displacement associated with the compatibility-restoring elastic equilibration, \mathbf{u}_c [1]; $1 - \mathbf{g} \leq \mathbf{0}$ the constraints which ensure that the growth is expansive, i.e. the elements, in this case, don't shrink; $\boldsymbol{\mu}$, $\boldsymbol{\alpha}$ and $\boldsymbol{\gamma}$ are the Lagrange multipliers corresponding to the constraints; \mathbf{K} is the global stiffness

matrix, which depends on the growth-displacement \mathbf{u}_g and the material properties; \mathbf{f} the global applied external load vector; $\mathbf{R}\mathbf{u}_c - \mathbf{d} = \mathbf{0}$ is the equation for compatibility restoring equilibration [1], wherein \mathbf{R} a constant that depends on the mesh-connectivity.

The Lagrangian for this problem is as follows,

$$L = \frac{(\Delta\mathbf{u})^T(\Delta\mathbf{u})}{2} + \boldsymbol{\mu}^T(\mathbf{K}\mathbf{u}_c - \mathbf{f} + \mathbf{R}^T\boldsymbol{\lambda}) + \boldsymbol{\alpha}^T(\mathbf{R}\mathbf{u}_c - \mathbf{d}) + \boldsymbol{\gamma}^T(1 - \mathbf{g}) \quad (6)$$

The necessary condition for the optimization problem gives:

$$\nabla_{\mathbf{g}}L = (\Delta\mathbf{u})^T \frac{\partial(\Delta\mathbf{u})}{\partial\mathbf{g}} + \boldsymbol{\mu}^T \left(\frac{\partial\mathbf{K}}{\partial\mathbf{g}} \mathbf{u}_c + \mathbf{K} \frac{\partial\mathbf{u}_c}{\partial\mathbf{g}} + \mathbf{R}^T \frac{\partial\boldsymbol{\lambda}}{\partial\mathbf{g}} \right) + \boldsymbol{\alpha}^T \left(\mathbf{R} \frac{\partial\mathbf{u}_c}{\partial\mathbf{g}} - \frac{\partial\mathbf{d}}{\partial\mathbf{g}} \right) - \boldsymbol{\gamma} = 0 \quad (7)$$

The Karush Kuhn Tucker (KKT) conditions corresponding to the inequality constraints in Eq. (5), are given by

$$\boldsymbol{\gamma}^T(1 - \mathbf{g}) = 0 \quad (8)$$

$$\boldsymbol{\gamma} \geq 0 \quad (9)$$

Collecting the terms that involve the gradients of the state-variables and known derivatives from Eq. (7), we get the following vector equation:

$$\begin{aligned} \nabla_{\mathbf{g}}L = & \left((\Delta\mathbf{u})^T + \boldsymbol{\mu}^T \mathbf{K} + \boldsymbol{\alpha}^T \mathbf{R} \right) \frac{\partial\mathbf{u}_c}{\partial\mathbf{g}} + \left(\boldsymbol{\mu}^T \mathbf{R}^T \right) \frac{\partial\boldsymbol{\lambda}}{\partial\mathbf{g}} - \boldsymbol{\alpha}^T \frac{\partial\mathbf{d}}{\partial\mathbf{g}} \\ & + (\Delta\mathbf{u})^T \frac{\partial\mathbf{u}_g}{\partial\mathbf{g}} + \boldsymbol{\mu}^T \frac{\partial\mathbf{K}}{\partial\mathbf{g}} \mathbf{u}_c - \boldsymbol{\gamma} = 0 \end{aligned} \quad (10)$$

We use the adjoint method to solve the preceding equation by setting to zero the terms involving the gradients of the state-variables with respect to the design variables as follows:

$$\begin{aligned} \mathbf{K}\boldsymbol{\mu} + (\Delta\mathbf{u})^T + \mathbf{R}^T\boldsymbol{\alpha} &= 0 \\ \mathbf{R}\boldsymbol{\mu} &= 0 \end{aligned} \quad (11)$$

which are similar in form to the constraint equations in Eq. (5).

The iterations in the optimization are performed so as to drive the set of equations given by Eq. (10) to zero. We start with an initial guess of unity for the growth-rates, i.e. $\mathbf{g}^0 = [1 \ \cdots \ 1]^T$, where the superscript indicates the iteration-

number. In each iteration, the displacements \mathbf{u}_g and \mathbf{u}_c corresponding to the current growth-rate \mathbf{g}^k are found. The Lagrange multipliers corresponding to these values were computed using the system of equations given by Eq. (11). Following this, the growth-rates were updated using the following update rule:

$$\mathbf{g}^{k+1} = \mathbf{g}^k + \beta (\nabla_{\mathbf{g}} L)^\eta \quad (12)$$

where \mathbf{g}^{k+1} and \mathbf{g}^k are the growth-rate vectors in the $(k+1)^{\text{th}}$ and k^{th} iterations respectively; β and η are parameters that dictate the step-size and the scaling respectively.

If the inequality constraints given in Eq. (5) are not violated, we proceeded with the next iteration. If these inequality constraints are violated, further iterations are performed in an inner loop, with the following update is performed:

$$\mathbf{g}_{m+1}^{k+1} = \begin{cases} \mathbf{g}_m^{k+1}, \mathbf{a} = \mathbf{0}, \text{ if } \mathbf{g}_m^{k+1} > 1 \\ 1, \mathbf{a} \neq \mathbf{0}, \text{ if } \mathbf{g}_m^{k+1} \leq 1 \end{cases} \quad (13)$$

where the subscripts indicate the inner iteration count. These inner iterations are performed until all the elemental growth-rates are pushed to 1 or all of them satisfy the constraints. These iterations are performed until the relative change in the relative change in the growth-rate vectors is less than a pre-defined value (which was taken to be 1%) or when the absolute value of the objective function is less than a $1e-10$.

In this work, since the updates in the algorithm require the global stiffness matrix and its derivatives, a Finite Element code was implemented in MathematicaTM (<http://www.wolfram.com/mathematica>). This code was first benchmarked against AbaqusTM (www.simulia.com/abaqus) before using in this work.

4.2 Results and Discussion

In this section, we discuss the results obtained from the inverse growth-problem run on images taken 5 days apart, as shown in Fig. (6). The images were first aligned, following which the locations of spots in both the images were extracted.

The displacements of the dots were extracted from the images, which was then used to estimate the growth-rate in the growing leaf. This growth-rate is visualized using a density plot in Fig. (7), with the darker regions indicating regions that are growing slower than the lighter regions. It was observed that when a different initial guess was used for the growth-rates, we obtain a different solution, suggesting a possibility of imposing additional biologically relevant constraints in Eq. (5) to narrow down the solution space.

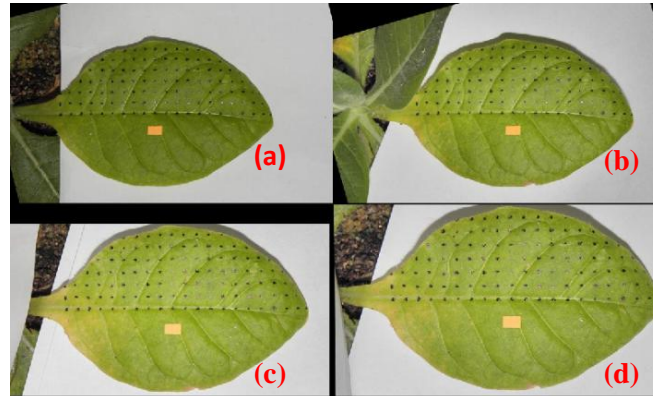


Figure 6: Images of the leaf taken during the first day, fifth day tenth day and fifteenth days shown in insets (a)-(d). The images have been processed so that the marker (orange colour), is of the same size in both the images and they occupy the same position in both the images. The spots (black dots) on the leaf lamina are then extracted from which the displacement of the each spot is computed. Following this, these displacements are used in the inverse growth problem to estimate the growth-rate of the leaf lamina.

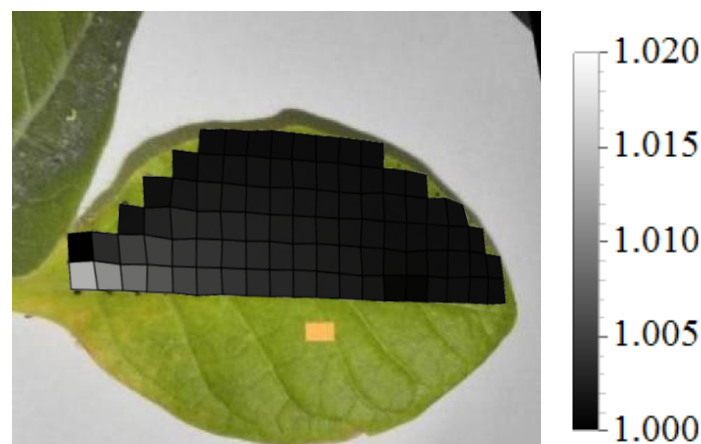


Figure 7: The growth-rates obtained from the inverse problem, shown overlaid on the aligned image of the leaf. In the density plot shown, the lighter regions grow faster than the darker regions. The growth-rate was estimated using the inverse problem by processing images that were one week apart.

Acknowledgements

This work was supported by the Math-Bio initiative from the Department of Bio-Technology (DBT) of the Government of India, which is gratefully acknowledged. We thank the students from Prof. Utpal Nath's lab, who helped us with the

experimental setup. Also, we thank Prabhakar N, for assisting us with the fabrication of the device and setting up the imaging system.

References

- [1] Ramnath Babu T.J., *A Discretized Approach to Modelling Growth with Application to A Shape-Matching Inverse Problem in Leaf-Growth*, PhD Thesis, Indian Institute of Science, Bangalore, 2014.
- [2] Schmundt, D., Stitt, M., Jähne, B., & Schurr, U. (1998). Quantitative analysis of the local rates of growth of dicot leaves at a high temporal and spatial resolution, using image sequence analysis. *The Plant Journal*, 16(4), 505-514.
- [3] Palmer, S. J., & Davies, W. J. (1996). An analysis of relative elemental growth rate, epidermal cell size and xyloglucan endotransglycosylase activity through the growing zone of ageing maize leaves. *Journal of Experimental Botany*, 47(3), 339-347.
- [4] Mielewczik, Michael, Michael Friedli, Norbert Kirchgessner, and Achim Walter. "Diel leaf growth of soybean: a novel method to analyze two-dimensional leaf expansion in high temporal resolution based on a marker tracking approach (Martrack Leaf)." *Plant methods* 9, no. 1 (2013): 1-14.
- [5] Yin, X., Liu, X., Chen, J., & Kramer, D. M. (2014, October). Multi-leaf tracking from fluorescence plant videos. In *Image Processing (ICIP), 2014 IEEE International Conference on* (pp. 408-412). IEEE.
- [6] Teng, C. H., Kuo, Y. T., & Chen, Y. S. (2009). Leaf segmentation, its 3d position estimation and leaf classification from a few images with very close viewpoints. In *Image Analysis and Recognition* (pp. 937-946). Springer Berlin Heidelberg.
- [7] De Vylder, J., Ochoa, D., Philips, W., Chaerle, L., & Van Der Straeten, D. (2011). Leaf segmentation and tracking using probabilistic parametric active contours. In *Computer Vision/Computer Graphics Collaboration Techniques* (pp. 75-85). Springer Berlin Heidelberg.
- [8] The Math Works, Image processing toolbox with Matlab v.4, Natick, MA., USA, The MathWorks.
- [9] Schalkoff, R. J. (1989). *Digital image processing and computer vision* (Vol. 286). New York: Wiley.
- [10] Ramnath Babu T. J. and G.K. Ananthasuresh, *Estimating the Growth-rate of a Leaf to attain its 2D Target Forms using Optimization*, OPT-i, June 2014.